Improved anti-tumor effect of liposomal doxorubicin after targeted blood-brain barrier disruption by MRI-guided focused ultrasound in rat glioma

Lisa H. Treat[1,2], **Nathan McDannold**[2,*], **Yongzhi Zhang**[2], **Natalia Vykhodtseva**[2], and **Kullervo Hynynen**[3]

[1]Harvard-MIT Division of Health Sciences and Technology, Cambridge, Massachusetts USA

[2]Radiology, Harvard Medical School and Brigham & Women's Hospital, Boston, Massachusetts USA

[3]Imaging Research, Sunnybrook Health Sciences Centre, University of Toronto, Toronto, Ontario Canada

Abstract

The blood-brain barrier (BBB) inhibits the entry of the majority of chemotherapeutic agents into the brain. Previous studies have illustrated the feasibility of drug delivery across the BBB using focused ultrasound (FUS) and microbubbles. Here, we investigated the effect of FUS-enhanced delivery of doxorubicin on survival in rats with and 9L gliosarcoma cells inoculated in the brain. Each rat received either: (1) no treatment (control; N=11), (2) FUS only (N=9), (3) i.v. liposomal doxorubicin (DOX only; N=17), or (4) FUS with concurrent i.v. injections of liposomal doxorubicin (FUS+DOX; N=20). Post-treatment MRI showed that FUS+DOX reduced tumor growth compared to DOX only. Further, we observed a modest but significant increase in median survival time after a single treatment FUS+DOX treatment (p=0.0007), whereas neither DOX nor FUS had any significant impact on survival on its own. These results suggest that combined ultrasound-mediated BBB disruption may significantly increase the antineoplastic efficacy of liposomal doxorubicin in the brain.

Keywords

focused ultrasound; blood-brain barrier; doxorubicin; 9L gliosarcoma; survival

Introduction

Aggressive malignancies of the central nervous system (CNS) are among the most difficult to treat due to the presence of the blood-brain barrier (BBB) (Gloeckler Ries et al. 2003; Lagerwaard et al. 1999; Surawicz et al. 1998). The restrictive permeability of the BBB prohibits the passage of many therapeutic agents from systemic circulation into brain parenchyma (Pardridge 2002; Banerjee and Bhat 2007) or prevents their accumulation at

*Correspondence to: Department of Radiology, Brigham and Women's Hospital, 221, Longwood Avenue, room 521, Boston, MA 02115. Fax: 617-525-7450. njm@bwh.harvard.edu.

Publisher's Disclaimer: This is a PDF file of an unedited manuscript that has been accepted for publication. As a service to our customers we are providing this early version of the manuscript. The manuscript will undergo copyediting, typesetting, and review of the resulting proof before it is published in its final citable form. Please note that during the production process errors may be discovered which could affect the content, and all legal disclaimers that apply to the journal pertain.

sufficient concentrations (von Holst et al. 1990). Although tumor vasculature is often malformed and the integrity of its BBB compromised, the complex problem of drug delivery to the brain persists. Because systemic chemotherapeutic agents are not able to penetrate solid tumors homogenously (Fukumura and Jain 2007), portions of the tumor are often left untreated or partially treated after traditional intravenous chemotherapy. Additionally, malignant cells may infiltrate the tumor margin where the BBB remains intact. Invisible to the surgeon and unreachable by pharmacological interventions, these infiltrating neoplastic cells are responsible for 78–90% of cases of recurrent glioma (Hochberg and Pruitt 1980; Wallner et al. 1989). Thus, the BBB remains a formidable obstacle in the treatment of patients with brain malignancies. Even with aggressive surgical resection and radiotherapy, the prognosis for the most common and most aggressive form of glioma in adults is associated with a median survival of less than one year from the time of diagnosis (Walker et al. 1978; DeAngelis 2001).

A novel approach to the problem of drug delivery to the brain uses focused ultrasound to temporarily disrupt the BBB in a noninvasive and localized manner (Hynynen et al. 2001). When applied to the brain in the presence of gas-filled microbubbles, high-frequency acoustic energy has been shown to stimulate active vesicular transport and transiently disassemble tight junctional complexes to allow the passage of molecules which would not otherwise penetrate the BBB (Sheikov et al. 2004; Sheikov et al. 2008). As the energy is tightly focused to diameters as small as <1 mm, its effects on the BBB can be confined to a limited volume of tissue to enable targeted therapy (Kinoshita et al. 2006a; Treat et al. 2007; Choi et al. 2007). In addition to its localized effects, focused ultrasound has the advantage of noninvasive application. While the use of ultrasound for brain applications has historically required the removal of the skull due to its strong attenuation in bone (Fry and Fry 1960; Heimburger 1985), experimental and theoretical studies have demonstrated that focused ultrasound could be applied through the skull without an invasive craniotomy using a phased transducer array (Hynynen and Jolesz 1998; Sun and Hynynen 1998) and correction factors derived from computed tomography (CT) scans (Clement and Hynynen 2002; Aubry et al. 2003). When guided by MRI, focused ultrasound can target precise anatomical structures in a completely noninvasive manner (Hynynen et al. 2006). Such devices have been tested clinically (McDannold et al. 2010; Martin et al. 2009).

The high spatial resolution and noninvasive nature of ultrasound-induced BBB disruption make it an advantageous technique for targeted drug delivery to the brain. The feasibility of trans-BBB delivery by focused ultrasound has been well established for numerous agents, including imaging fluorophores (Raymond et al. 2007), Herceptin (Kinoshita et al. 2006a), liposomal doxorubicin (DOX) (Treat et al. 2007), methotrexate (Mei et al. 2009), Alzheimer's disease immunotherapeutics (Raymond et al. 2008), and other antibodies (Kinoshita et al. 2006b). Recent studies have also demonstrated that enhanced delivery via ultrasound-induced BBB disruption can improve outcomes in animal models for glioma (Liu et al. 2010) and Alzheimer's disease (Jordao et al. 2010).

Doxorubicin has been shown to be effective against malignant glioma both *in vitro* (Stan et al. 1999) and *in vivo* when injected directly into the tumor (Walter et al. 1995; Voulgaris et al. 2002). One study confirmed that ultrasound-enhanced delivery of DOX to the normal rat brain makes it possible to achieve tissue drug concentrations at levels sufficient to have a therapeutic effect in humans, with 3- to 20-fold increases in drug concentrations in sonicated regions of the brain compared non-targeted regions (Treat et al. 2007). Furthermore, it has been shown that ultrasound may be used to enhance intracellular delivery and synergistically increase the efficacy of other chemotherapeutic agents in glioma cells *in vitro* (Zarnitsyn et al. 2007). However, such a therapeutic benefit has not yet been demonstrated *in vivo*. In the

present study, we examined the impact of focused-ultrasound enhanced chemotherapy on survival in an *in vivo* rodent model of aggressive glioma.

Materials and Methods

Cell culture

9L gliosarcoma cells were obtained from the University of California–San Francisco/ Neurosurgery Tissue Bank. Cells were cultivated in Minimum Essential Medium with Earle's salts, supplemented with 10% fetal calf serum, 1% L-glutamine, 1% MEM nonessential amino acids, and 0.1% gentamicin (10% FCS-MEM) in a 5% CO_2 chamber held at 37 deg C.

Animals

Male Sprague-Dawley rats (~200 g) were acquired from Charles River Laboratories (Boston, Massachusetts). For surgery or experiments involving exposure to ultrasound (sonication), rats were anesthetized by i.p. administration of ketamine (90 mg/kg) and xylazine (10 mg/kg) per hour or as needed. For imaging on days before or after ultrasound exposure, rats were anesthetized by induction in a vaporized isofluorane chamber (3% induction, 1–2% maintenance). In preparation for surgery or sonication, the hair covering the dorsal surface of the skull was removed with depilatory lotion. For experiments requiring i.v. administration of contrast agents or chemotherapy, a 24-gauge catheter was inserted into the tail vein.

All animals were cared for in accordance with our institutional animal care policy. Euthanasia of animals exhibiting severely impaired activity or weight loss in excess of 20% was conducted on animals under deep anesthesia by i.p. injection of sodium pentobarbital (Euthasol, 180 mg/kg; Virbac Corporation, Fort Worth, Texas) or by transcardial perfusion with 0.9% NaCl solution and 10% formalin in 0.1 M phosphate buffer to preserve the brain/ tumor structure for histological analysis.

Tumor implantation

In the anesthetized rat, the dorsal surface of the skull was sterilized with an iodine swab. A 1-cm linear skin incision was placed over the bregma and a 1-mm burr hole was drilled into the skull approximately 2 mm lateral to the bregma. A 10-μL gas-tight syringe (Hamilton, Reno, Nevada) was used to inject $(0.5–1) \times 10^5$ 9L rat gliosarcoma (9L GL) cells suspended in 2–4 μL 10% FCS-MEM into the right or left frontal lobe at a depth of 3.5 mm relative to the dural surface of the brain. To minimize convection at the injection site, the cell suspension was slowly injected over 5 min. Two minutes after injection, the needle was slowly retracted over an additional 5 min. The wound was rinsed with 0.9% NaCl solution and the burr hole occluded with sterile bone wax (Ethicon, Somerville, New Jersey) to prevent leakage of the cerebrospinal fluid. The skin was then closed with 5-0 silk sutures (Ethicon, Somerville, New Jersey) and the rat allowed to recover from anesthesia under observation. Each animal was given a one-time dose by i.p. administration of antibiotic (Baytril, 2.5 mg/kg; Bayer HealthCare, Wayne, New Jersey) and analgesic (Buprenex, 0.05 mg/kg; Reckitt Benckiser Healthcare, Hull, England, UK) every 12 h for 24 h following surgery. Sutures were removed prior to sonication, usually 5 days after surgery. MR images of the brain were acquired 7 or 8 days following implantation. Animals were included in the study if the tumor appeared to be well-circumscribed and if the larger cross3 sectional diameter was within 1–3 mm, inclusive.

Study design

On Day 8 after implantation, each rat was randomly assigned to one of the following groups: (1) no treatment (control; N=11), (2) a single treatment with microbubble-enhanced MRI-guided focused ultrasound (FUS only; N=9), (3) a single treatment with i.v. liposomal doxorubicin (DOX only; N=17), or (4) a single treatment with microbubble-enhanced MRI-guided focused ultrasound and concurrent i.v. injections of liposomal doxorubicin (FUS+DOX; N=20). Additional MR images of the brain were acquired weekly to monitor tumor growth. Animals were followed until death, up to 55 days. Total survival times from tumor implantation until death were recorded. Six additional animals had implanted tumors with growth rates that were clearly different than the others, suggesting problematic tumor cell preparation or implantation. These animals were considered outliers and excluded from the study.

Ultrasound

Ultrasonic waves (sonications) were generated by a single-element focused transducer (diameter = 10 cm; radius of curvature = 8 cm; frequency = 1.7 MHz, ellipsoid focal spot with half-maximum pressure amplitude diameter/length, in water: 1 mm/4 mm) whose electrical impedance was matched to 50 Ohms. The transducer was mounted on an MRI-compatible manual positioning device with three translational degrees of freedom and immersed in a tank of degassed water integrated into the table of a standard clinical MRI scanner (Fig. 1*A*). An external network consisting of an RF power amplifier (50-dB gain, E&I model #240L, Rochester, New York), function generator (Fluke Corporation, Everett, Washington), and personal computer was used to control sonication. Prior to each animal experiment, MR images were acquired during high-power continuous-wave sonications in a gel phantom to determine the coordinates of the acoustic focus of the transducer.

For animals in Groups 2 (FUS only) and 4 (FUS+DOX) which received treatment with microbubble-enhanced MRI-guided focused ultrasound, each rat was laid supine over the water tank so that the dorsal surface of its head was acoustically coupled to the transducer with degassed water (P_O_2 <1 ppm). Pre-sonication images of the brain were acquired to determine the size and coordinates of the tumor. The transducer was repositioned to align its focus with the tumor, which was then exposed to pulsed ultrasound (derated pressure amplitude: 1.2 MPa, burst length: 10 ms, pulse repetition frequency: 1 Hz, duration: 60–120 s; sonication repeated every 5 min in overlapping square pattern; see ref (Treat et al. 2007) for further detail). Ultrasonographic contrast agent (Definity, 0.01–0.02 mL/kg; Lantheus Medical Imaging, North Billerica, MA, USA) consisting of perflutren lipid microspheres (mean diameter, 1.1–3.3 μm) was diluted to 10% normal strength (maximum concentration after dilution, 1.2×10^9 bubbles per mL) with a solution of 0.01 M phosphate buffer, 0.0027 M KCl, and 0.137 M NaCl. The dose of contrast agent per sonication was selected to be similar to the 0.01 mL/kg dose recommended for clinical ultrasound imaging. At the start of sonication, a bolus of the diluted contrast agent was injected simultaneously into the catheterized tail vein, followed by a 0.2-mL flush with 0.9% NaCl solution. The transducer was then moved to its new position and the procedure repeated every 5 min until the entire projected area of the tumor and its margins had been exposed to the acoustic focus, usually 5–9 sonications in total with the 1-mm spacing. Contrast-enhanced MR images were obtained immediately following the first two exposures, which were aimed 1 mm outside of the tumor, to confirm the *in vivo* location of the acoustic focus relative to the tumor prior to treatment.

Chemotherapy

Animals in Groups 3 (DOX only) and 4 (FUS+DOX) received single-agent intravenous administration of doxorubicin hydrochloride encapsulated in long-circulating pegylated

liposomes (Doxil; Ortho-Biotech, Bridgewater, New Jersey). In this form, greater than 90% of the drug is contained within the liposomes (~100 nm). Each rat was administered 5 slow bolus injections of DOX followed by 0.2 mL 0.9% NaCl solution into the catheterized tail vein at 5-min intervals, for a total dose of 5.67 mg/kg. For the animals in Group 4, the DOX injections immediately followed the administration of Definity microbubble contrast agent so that the concurrent ultrasound exposure may enhance the release of the DOX from the liposomes in the localized region of focal BBB disruption.

Magnetic resonance imaging

Magnetic resonance images of the brain were acquired in all animals for guidance and evaluation. For animals in Groups 2 (FUS only) and 4 (FUS+DOX), the ultrasound experimental set-up (Fig. 1A) was integrated into the table of a 3.0-Tesla clinical MRI scanner (Signa; GE Healthcare, Milwaukee, Wisconsin). A 7.5-cm-diameter transmit/receive surface coil was centered on the dorsal surface of the head. Two-dimensional T2-weighted fast spin-echo (FSE) images of the brain (repetition/echo time: 2000/91 ms; echo train length: 8; image matrix: 256×256; slice thickness/spacing: 1.5 mm/interleaved; field of view: 8 cm; number of excitations: 2; flip angle: 90 deg) were acquired in three orthogonal planes to determine the size and location of the tumor. To show the baseline contrast enhancement of the tumor prior to ultrasound exposure (Fig. 1B, left), two-dimensional T1-weighted FSE images of the tumor (repetition/echo time: 500/13 ms; echo train length: 4; image matrix: 256×256; slice thickness: 1.5 mm; field of view: 8 cm; number of excitations: 4; flip angle: 90 deg) were acquired in the plane perpendicular to the direction of ultrasound propagation and then repeated after i.v. administration of gadopentatate dimeglumine MR contrast agent (Magnevist; Bayer HealthCare, Wayne, New Jersey; 0.25 mL/kg). The target site for BBB disruption was selected on the MR images and the transducer repositioned accordingly. Sonications were performed through the opening of the surface coil, which was filled with a plastic bag [poly(vinyl chloride), thickness ~75 μm] containing degassed water. After treatment with ultrasound was completed, additional contrast-enhanced T1-weighted FSE images were acquired to confirm successful ultrasound-induced BBB disruption in and around the tumor (Fig. 1B, right).

Additional T2-weighted rapid acquisition with relaxation enhancement (RARE) images of the brain (repetition/echo time: 2000/85 ms; echo train length: 8; image matrix: 256×256; slice thickness: 1.5 mm; field of view: 8 cm; number of excitations: 2; flip angle: 180 deg) were acquired in all animals using a 4.7-Tesla small animal MRI scanner (BioSpec Avance; Bruker, Billerica, Massachusetts).

Image analysis

The size of the tumor was evaluated with image analysis software written in-house using MATLAB (MathWorks, Natick, MA). Tumor volumes V were calculated using an ellipsoid approximation [$V \approx 4/3 * \pi * (0.5)^3 * (abc)$], where a, b, and c are the maximum diameters of the tumor measured in three orthogonal planes on two-dimensional T2-weighted MR images. Least-squares nonlinear regression analyses were performed to compare the rate of tumor growth between groups. For animals for which MRI data were acquired on at least 3 different days, tumor volumes were fit using an exponential model of the form $V = A*\exp(kt)$, where A and k are constant parameters and t is the number of days after implantation. Tumor volume doubling time $T\_1/2$ was then calculated for each animal using the equation $T\_1/2 = \ln(2)/k$.

Survival analysis

Population survival curves were also plotted using the Kaplan-Meier method (Kaplan and Meier 1958). Survival curves were compared between groups using the Log-Rank test.

Statistical analyses were performed using either GraphPad Prism version 5.01 for Windows (GraphPad Software, San Diego, California) or Excel 2002 (Microsoft Corporation, Redmond, Washington). The Bonferroni method was used to compare multiple pairs of groups (Bland and Altman 1995). The significance level for the family of comparisons was set at 0.05. Since there are four treatment groups (including control) with six possible paired comparisons, pairwise p values less than the Bonferroni-corrected threshold of $0.05/6 = 0.0083$ were considered statistically significant.

Histologic analysis

For illustrative purposes, the brains of three animals were examined to compare the histologic effects of different treatments. As with those in the survival study, these animals were randomly assigned on post-implantation Day 8 to one of Groups 1 (control), 3 (DOX only), or 4 (FUS+DOX). Forty-eight hours after treatment, the animals were euthanized by transcardiac perfusion with 0.9% NaCl solution followed by 10% phosphate-buffered formalin while under deep anesthesia with ketamine and xylazine. Their brains were harvested and fixed in formalin; tissue blocks containing the tumor were embedded in paraffin and cut into 6-μm serial sections perpendicular to the direction of ultrasound propagation. Every thirtieth section was stained with hemotoxylin and eosin (H&E) for examination by light microscopy.

Results

Delayed tumor growth in rats treated with ultrasound-enhanced chemotherapy

Images of the brain obtained weekly before and after treatment were used to compare the effects of each treatment on glioma growth rate. Fig. 2 shows an example of T2-weighted MR images of the brain of a rat treated with FUS+DOX and of one treated with DOX only. On a week-by-week basis, the rat treated with FUS+DOX seemed to exhibit a tumor growth pattern comparable to that of the rat treated with DOX only until two weeks after treatment, when noticeable differences in the growth patterns emerged. While the tumor in the DOX-only-treated rat continued to grow exponentially ($R^2 = 0.999$) even after treatment, tumor growth in the FUS+DOX-treated rat was visibly delayed, allowing the ultrasound-enhanced treated rat to survive longer.

Exponential growth time constants for each rat were calculated from least-squares regression analyses. Animals treated with FUS+DOX exhibited an average tumor volume doubling time ($T\_1/2 \pm$ SD) of 3.7 ± 0.5 days, whereas those treated with DOX only had a doubling time $T\_1/2 = 2.7 \pm 0.4$ days. Animals who received FUS only or no treatment exhibited similar tumor growth rates as the latter group with $T\_1/2 = 2.2 \pm 0.3$ days and $T\_1/2 = 2.3 \pm 0.3$ days, respectively. These results confirmed that rats treated with FUS+DOX had longer average tumor volume doubling times than any other group (Fig. 3). In all cases except one, the coefficient of determination R^2 of the exponential fit exceeded 0.94. One animal treated with FUS+DOX was excluded from the calculation of the average doubling time ($T\_1/2 = 7.9$ days) because its tumor growth pattern after FUS+DOX treatment was not well described by an exponential fit ($R^2 = 0.44$).

Improved survival in rats treated with ultrasound-enhanced chemotherapy

To further investigate the therapeutic efficacy of ultrasound-enhanced chemotherapy, we compared the population survival curves between groups of rats with implanted 9L gliosarcoma tumors which received different treatments. Fig. 4 shows the Kaplan-Meier estimates of survival in rats for the four experimental groups. Six animals treated with FUS (either by itself or in combination with DOX) did not recover after treatment, possibly due

to prolonged time under anesthesia; these animals are considered lost to follow-up (censored) after Day 8.

The results of the survival analysis are listed in Table 1. The median survival times for each group were 25, 25, 29, and 31 days, respectively. The Log-Rank test for the groups 2, 3, and 4 compared to the nontreated reference group yields $X^2 = 1.25$ ($p = 0.26$), 1.86 ($p = 0.17$), and 11.61 ($p = 0.0007$), respectively. Thus, rats which received a single treatment of FUS +DOX had a 24% greater median survival time than nontreated rats, and the difference was highly significant ($p = 0.0007$). In contrast, rats which received DOX only had a 16% greater median survival time than nontreated rats, but the difference was not statistically significant ($p = 0.17$). In addition, the proportion of long-term (> 40 days) survivors in the FUS+DOX group was 26.7%, whereas no rats in the other three groups survived beyond 34 days. There was no significant difference in survival between animals treated with FUS only and nontreated controls.

Histologic analysis

Preliminary histological evaluation of representative brains from animals with implanted 9L gliosarcoma showed marked differences at the edge of tumors treated with FUS+DOX compared to those treated with DOX only (Fig. 5). At 48 h after treatment, the edge of the tumor treated with FUS+DOX was characterized by parenchymal vacuolation and damaged tumor cells. (Fig. 5*A, B*, arrow). In the animals treated with DOX only, the tumor edges remained intact and undamaged infiltrating tumor cells were visible in the tissue beyond the solid tumor and surrounding an intact blood vessel (Fig. 5*C, D*, arrows).

Discussion

Doxorubicin (formerly known as adriamycin) is a ubiquitous antineoplastic agent used in both single-agent and combination chemotherapy. It has been shown to be effective against malignant glioma both *in vitro* (Stan et al. 1999) and *in vivo* when injected directly into the tumor (Walter et al. 1995; Voulgaris et al. 2002). However, systemic administration of this potent cytotoxic agent results in poor accumulation in glioma tissue because it does not readily cross the intact BBB (von Holst et al. 1990). Thus, while DOX is widely used to treat extracranial cancers, it has been ineffective against malignancies within the brain, in spite of the enhanced penetration and retention effect of pegylated liposomes in tumors. The evidence suggests that if the agent had a means of penetrating the BBB and its accumulation in the tumor could be increased to therapeutic levels, then its clinical use could have a profound impact on survival in patients afflicted with primary or metastatic brain tumors.

In a previous study of drug quantification, we demonstrated that it is possible to achieve therapeutic levels of DOX in localized areas of the brain by using MRI-guided focused ultrasound to induce transient BBB disruption in rats (Treat et al. 2007). In the present study of therapeutic impact, we have shown that a combined treatment of ultrasound-induced focal BBB disruption and i.v. DOX significantly improves survival and slows disease progression in rats with aggressive glioma. Rats who received ultrasound-enhanced chemotherapy showed a modest but highly significant increase in median survival time, as well as an increase in the proportion of long-term survivors, compared to those who received stand-alone chemotherapy. In addition, follow-up MRI confirmed that rats who received the combined treatment experienced slower tumor growth with increased tumor volume doubling times. Not surprisingly, rats treated with only intravenous DOX exhibited no significant difference in survival from those who did not receive any treatment. Similarly, rats treated with only microbubble-enhanced focused ultrasound showed no significant difference in survival from the control group. Thus, neither ultrasound nor intravenous

chemotherapy was sufficient on its own to achieve the improved survival benefit observed when the two treatments were combined.

The enhanced therapeutic efficacy of the combined treatment may be attributable to augmented localized release of DOX from disrupted liposomes in the focal target and the increased penetration of the drug through the ultrasound-induced BBB disruption. The interaction of low-power focused ultrasound with intravascular microbubbles is thought induce mechanical stresses on the brain microvascular endothelial wall, which induce focal and transient BBB opening (Hynynen et al. 2001). Immunoelectron microscopy studies in normal brain indicate that passage through the BBB after treatment with microbubble-enhanced ultrasound occurs via both paracellular and transcellular routes, including (1) open endothelial cell tight junctions (TJ), (2) enhanced active vesicular transport, (3) endothelial cell fenestration and channel formation, and (4) free passage through injured endothelium (Sheikov et al. 2004; Sheikov et al. 2006). Specifically, the redistribution and loss of immunosignals for TJ-specific proteins occludin, claudin-5, and ZO-1 provide direct evidence of the disassembling of the TJ molecular structure and associated functional loss of the BBB immediately following ultrasound exposure; six hours after sonication, the protein immunosignals and BBB function are both restored (Sheikov et al. 2008). We note that these mechanisms of ultrasound-mediated BBB disruption elucidated in the normal brain may not all be identical to those in glioma, in which the vasculature is immature, variably permeable, and inhomogeneously distributed. Differences in vasculature distribution and functionality in tumors may account in part for the modest effect of the ultrasound- mediated drug delivery observed in this study, compared to the markedly enhanced drug penetration in normal brain (Treat et al. 2007). It remains to be explored whether and how the effects of microbubble-enhanced focused ultrasound in neoplastic tissue differs from its effects in normal brain tissue. Only limited histological examination on representative examples from the different groups was performed in this pilot study. Future work is needed to examine a larger sample size, and to evaluate the effects of these treatments at different time-points to elucidate such effects and to examine the effects focused ultrasound, DOX, and their combination in tumors.

It is arguable that the effects that we did observe with histology at the tumor margins may have contributed to the slowed tumor growth and increased survival times observed in rats treated with ultrasound-enhanced chemotherapy. Vacuolation in the tumor margin may have inhibited growth at its proliferative edge. It is also plausible that since the periphery of the tumor typically contains more functional blood vessels than its core, greater DOX delivery by the ultrasound-mediated BBB disruption may have contributed to greater effects observed in these regions. However, since animals who received ultrasound without chemotherapy exhibited no significant difference in survival from nontreated control animals, we believe that the ultrasound in itself would be an unlikely explanation of the improved survival effect that we observed. It is more likely that the therapeutic benefit of the ultrasound-enhanced treatment resulted primarily from the increased penetration of DOX across the BBB and its accumulation in and around the tumor, thus improving the antitumoral efficacy of the systemic agent. Furthermore, previous studies of focused ultrasound with Optison microbubble contrast agent in normal brain tissue have shown that it is possible to achieve BBB disruption without significant histologic effects over a one-month follow-up period (McDannold et al. 2005). In these studies, only minor capillary extravasation of erythrocytes after acute exposure was observed. Although the effects observed with histology in the current study were more severe than in previous studies, it should be noted that the ultrasound protocol used in this study of therapeutic efficacy has not yet been optimized for drug delivery. In addition, extensive parametric studies on the threshold for tissue damage using focused ultrasound and Definity microbubble contrast agent have not yet been performed.

The role of chemotherapy in the treatment of patients with brain tumors has been controversial. Individual randomized controlled clinical trials of the use of single-agent or multi-agent chemotherapy in addition to cranial irradiation have failed to demonstrate any significant improvement in median survival. However, meta-analysis has shown a significant difference in median survival in brain tumor patients who receive chemotherapy (Fine et al. 1993). Although the effect of chemotherapy on median survival is controversial, there is little doubt that chemotherapy significantly increases the proportion of long-term survivors from less than 5 percent to approximately 15–20 percent (DeAngelis et al. 1998). This finding has been consistent across trials (DeAngelis 2001) and is consistent with our current results. Recent developments in the identification of genetic markers linked to chemotherapeutic response (Cairncross et al. 1998; van den Bent et al. 2006) have renewed interest in the use of chemotherapy for brain tumors with agents which can cross the BBB, such as temozolomide. The development of focused ultrasound-induced BBB disruption as a noninvasive method for targeted drug delivery to the brain could further reinvigorate the field by opening the door to a wide spectrum of potential neurotherapeutics which may otherwise be ruled out based on their current inability to penetrate the BBB.

The advantages of using focused ultrasound to induce BBB disruption as a technique for drug delivery to the brain are numerous. Focused ultrasound-induced BBB disruption is temporary, noninvasive, spatially resolved, and generically applicable for the delivery of agents of a wide range of molecular size (up to ~150 kDa) (Kinoshita et al. 2006a; Raymond et al. 2007; Sheikov et al. 2006). While previous studies have illustrated the feasibility of drug delivery across the BBB using MRI-guided focused ultrasound, to our knowledge, this study is the first to demonstrate its therapeutic benefit *in vivo*. Although the increase in survival time is modest, it should be noted that it is achieved here with only a single treatment with ultrasound and a single dose of doxorubicin, whereas a typical chemotherapy regimen consists of multiple doses over time. We postulate that the therapeutic benefit of MRI-guided focused ultrasound-enhanced chemotherapy could be increased with repeated administration. Since the BBB disruption induced by focused ultrasound has been shown to be transient and reversible (Hynynen et al. 2005), repeated use of this technique in the clinical setting should be possible. The development of this technique for drug delivery across the BBB and other blood-CNS barriers would have innumerable clinical applications, including but not limited to malignant glioma. Our *in vivo* demonstration of the increased antitumoral efficacy of doxorubicin as a result of ultrasound-mediated delivery represents a major milestone in the development of this technique for neuropharmacological applications.

Conclusions

A single treatment with ultrasound-mediated BBB disruption to enhance local delivery of liposomal doxorubicin was shown to slow tumor growth and improve survival in an aggressive rat glioma model. These results suggest that this approach may significantly increase the antineoplastic efficacy of the cytotoxic agent in the brain. This *in vivo* demonstration of the therapeutic benefit of combined MRI-guided focused ultrasound-enhanced chemotherapy, achieved here with a single treatment, is an important step forward in the development of this technique for the improved treatment of patients with CNS malignancies.

Acknowledgments

family. Cell cultures (9L GL) were kindly provided by the University of California–San Francisco/Neurosurgery Tissue Bank.

Reference List

Aubry JF, Tanter M, Pernot M, Thomas JL, Fink M. Experimental demonstration of noninvasive transskull adaptive focusing based on prior computed tomography scans. J Acoust Soc Am. 2003; 113:84–93. [PubMed: 12558249]

Banerjee S, Bhat MA. Neuron-glial interactions in blood-brain barrier formation. Annu Rev Neurosci. 2007; 30:235–258. [PubMed: 17506642]

Bland JM, Altman DG. Multiple significance tests: the Bonferroni method. BMJ. 1995; 310:170. [PubMed: 7833759]

Cairncross JG, Ueki K, Zlatescu MC, Lisle DK, Finkelstein DM, Hammond RR, Silver JS, Stark PC, Macdonald DR, Ino Y, et al. Specific genetic predictors of chemotherapeutic response and survival in patients with anaplastic oligodendrogliomas. J Natl Cancer Inst. 1998; 90:1473–1479. [PubMed: 9776413]

Choi JJ, Pernot M, Small SA, Konofagou EE. Noninvasive, transcranial and localized opening of the blood-brain barrier using focused ultrasound in mice. Ultrasound Med Biol. 2007; 33:95–104. [PubMed: 17189051]

Clement GT, Hynynen K. A non-invasive method for focusing ultrasound through the human skull. Phys Med Biol. 2002; 47:1219–1236. [PubMed: 12030552]

DeAngelis LM. Brain tumors. N Engl J Med. 2001; 344:114–123. [PubMed: 11150363]

DeAngelis LM, Burger PC, Green SB, Cairncross JG. Malignant glioma: who benefits from adjuvant chemotherapy? Ann Neurol. 1998; 44:691–695. [PubMed: 9778271]

Fine HA, Dear KB, Loeffler JS, Black PM, Canellos GP. Meta-analysis of radiation therapy with and without adjuvant chemotherapy for malignant gliomas in adults. Cancer. 1993; 71:2585–2597. [PubMed: 8453582]

Fry WJ, Fry FJ. Fundamental neurological research and human neurosurgery using intense ultrasound. IRE Trans Med Electron. 1960; ME-7:166–181. [PubMed: 13702332]

Fukumura D, Jain RK. Tumor microenvironment abnormalities: causes, consequences, and strategies to normalize. J Cell Biochem. 2007; 101:937–949. [PubMed: 17171643]

Gloeckler Ries LA, Reichman ME, Lewis DR, Hankey BF, Edwards BK. Cancer survival and incidence from the Surveillance, Epidemiology, and End Results (SEER) program. Oncologist. 2003; 8:541–552. [PubMed: 14657533]

Heimburger RF. Ultrasound augmentation of central nervous system tumor therapy. Indiana Med. 1985; 78:469–476. [PubMed: 4020091]

Hochberg FH, Pruitt A. Assumptions in the radiotherapy of glioblastoma. Neurology. 1980; 30:907–911. [PubMed: 6252514]

Hynynen K, Jolesz FA. Demonstration of potential noninvasive ultrasound brain therapy through an intact skull. Ultrasound Med Biol. 1998; 24:275–283. [PubMed: 9550186]

Hynynen K, McDannold N, Clement G, Jolesz FA, Zadicario E, Killiany R, Moore T, Rosen D. Pre-clinical testing of a phased array ultrasound system for MRI-guided noninvasive surgery of the brain-A primate study. Eur J Radiol. 2006

Hynynen K, McDannold N, Sheikov NA, Jolesz FA, Vykhodtseva N. Local and reversible blood-brain barrier disruption by noninvasive focused ultrasound at frequencies suitable for trans-skull sonications. Neuroimage. 2005; 24:12–20. [PubMed: 15588592]

Hynynen K, McDannold N, Vykhodtseva N, Jolesz FA. Noninvasive MR imaging-guided focal opening of the blood-brain barrier in rabbits. Radiology. 2001; 220:640–646. [PubMed: 11526261]

Jordao JF, Ayala-Grosso CA, Markham K, Huang Y, Chopra R, McLaurin J, Hynynen K, Aubert I. Antibodies targeted to the brain with image-guided focused ultrasound reduces amyloid-beta plaque load in the TgCRND8 mouse model of Alzheimer's disease. PLoS ONE. 2010; 5:e10549. [PubMed: 20485502]

Kaplan EL, Meier P. Nonparametric estimation from incomplete observations. J Am Stat Assoc. 1958; 53:457–481.

Kinoshita M, McDannold N, Jolesz FA, Hynynen K. Noninvasive localized delivery of Herceptin to the mouse brain by MRI-guided focused ultrasound-induced blood-brain barrier disruption. Proc Natl Acad Sci U S A. 2006a; 103:11719–11723. [PubMed: 16868082]

Kinoshita M, McDannold N, Jolesz FA, Hynynen K. Targeted delivery of antibodies through the blood-brain barrier by MRI-guided focused ultrasound. Biochem Biophys Res Commun. 2006b; 340:1085–1090. [PubMed: 16403441]

Lagerwaard FJ, Levendag PC, Nowak PJ, Eijkenboom WM, Hanssens PE, Schmitz PI. Identification of prognostic factors in patients with brain metastases: a review of 1292 patients. Int J Radiat Oncol Biol Phys. 1999; 43:795–803. [PubMed: 10098435]

Liu HL, Hua MY, Chen PY, Chu PC, Pan CH, Yang HW, Huang CY, Wang JJ, Yen TC, Wei KC. Blood-brain barrier disruption with focused ultrasound enhances delivery of chemotherapeutic drugs for glioblastoma treatment. Radiology. 2010; 255:415–425. [PubMed: 20413754]

Martin E, Jeanmonod D, Morel A, Zadicario E, Werner B. High-intensity focused ultrasound for noninvasive functional neurosurgery. Ann Neurol. 2009; 66:858–861. [PubMed: 20033983]

McDannold N, Clement GT, Black P, Jolesz F, Hynynen K. Transcranial magnetic resonance imaging-guided focused ultrasound surgery of brain tumors: initial findings in 3 patients. Neurosurgery. 2010; 66:323–332. [PubMed: 20087132]

McDannold N, Vykhodtseva N, Raymond S, Jolesz FA, Hynynen K. MRI-guided targeted blood-brain barrier disruption with focused ultrasound: Histological findings in rabbits. Ultrasound Med Biol. 2005; 31:1527–1537. [PubMed: 16286030]

Mei J, Cheng Y, Song Y, Yang Y, Wang F, Liu Y, Wang Z. Experimental study on targeted methotrexate delivery to the rabbit brain via magnetic resonance imaging-guided focused ultrasound. J Ultrasound Med. 2009; 28:871–880. [PubMed: 19546329]

Pardridge WM. Drug and gene delivery to the brain: the vascular route. Neuron. 2002; 36:555–558. [PubMed: 12441045]

Raymond SB, Skoch J, Hynynen K, Bacskai BJ. Multiphoton imaging of ultrasound/Optison mediated cerebrovascular effects in vivo. J Cereb Blood Flow Metab. 2007; 27:393–403. [PubMed: 16685254]

Raymond SB, Treat LH, Dewey JD, McDannold N, Hynynen K, Bacskai BJ. Ultrasound enhanced delivery of molecular imaging and therapeutic agents in Alzheimer's disease mouse models. PLoS ONE. 2008; 3:e2175. [PubMed: 18478109]

Sheikov N, McDannold N, Jolesz F, Zhang YZ, Tam K, Hynynen K. Brain arterioles show more active vesicular transport of blood-borne tracer molecules than capillaries and venules after focused ultrasound-evoked opening of the blood-brain barrier. Ultrasound Med Biol. 2006; 32:1399–1409. [PubMed: 16965980]

Sheikov N, McDannold N, Sharma S, Hynynen K. Effect of Focused Ultrasound Applied With an Ultrasound Contrast Agent on the Tight Junctional Integrity of the Brain Microvascular Endothelium. Ultrasound Med Biol. 2008; 34:1093–1104. [PubMed: 18378064]

Sheikov N, McDannold N, Vykhodtseva N, Jolesz F, Hynynen K. Cellular mechanisms of the blood-brain barrier opening induced by ultrasound in presence of microbubbles. Ultrasound Med Biol. 2004; 30:979–989. [PubMed: 15313330]

Stan AC, Casares S, Radu D, Walter GF, Brumeanu TD. Doxorubicin-induced cell death in highly invasive human gliomas. Anticancer Res. 1999; 19:941–950. [PubMed: 10368637]

Sun J, Hynynen K. Focusing of therapeutic ultrasound through a human skull: a numerical study. J Acoust Soc Am. 1998; 104:1705–1715. [PubMed: 9745750]

Surawicz TS, Davis F, Freels S, Laws ER Jr, Menck HR. Brain tumor survival: results from the National Cancer Data Base. J Neurooncol. 1998; 40:151–160. [PubMed: 9892097]

Treat LH, McDannold N, Zhang Y, Vykhodtseva N, Hynynen K. Targeted delivery of doxorubicin to the rat brain at therapeutic levels using MRI-guided focused ultrasound. Int J Cancer. 2007; 121:901–907. [PubMed: 17437269]

van den Bent MJ, Hegi ME, Stupp R. Recent developments in the use of chemotherapy in brain tumours. Eur J Cancer. 2006; 42:582–588. [PubMed: 16427778]

von Holst H, Knochenhauer E, Blomgren H, Collins VP, Ehn L, Lindquist M, Noren G, Peterson C. Uptake of adriamycin in tumour and surrounding brain tissue in patients with malignant gliomas. Acta Neurochir (Wien). 1990; 104:13–16. [PubMed: 2386084]

Voulgaris S, Partheni M, Karamouzis M, Dimopoulos P, Papadakis N, Kalofonos HP. Intratumoral doxorubicin in patients with malignant brain gliomas. Am J Clin Oncol. 2002; 25:60–64. [PubMed: 11823699]

Walker MD, Alexander E Jr, Hunt WE, MacCarty CS, Mahaley MS Jr, Mealey J Jr, Norrell HA, Owens G, Ransohoff J, Wilson CB, et al. Evaluation of BCNU and/or radiotherapy in the treatment of anaplastic gliomas. A cooperative clinical trial. J Neurosurg. 1978; 49:333–343. [PubMed: 355604]

Wallner KE, Galicich JH, Krol G, Arbit E, Malkin MG. Patterns of failure following treatment for glioblastoma multiforme and anaplastic astrocytoma. Int J Radiat Oncol Biol Phys. 1989; 16:1405–1409. [PubMed: 2542195]

Walter KA, Tamargo RJ, Olivi A, Burger PC, Brem H. Intratumoral chemotherapy. Neurosurgery. 1995; 37:1128–1145. [PubMed: 8584154]

Zarnitsyn VG, Kamaev PP, Prausnitz MR. Ultrasound-enhanced chemotherapy and gene delivery for glioma cells. Technol Cancer Res Treat. 2007; 6:433–442. [PubMed: 17877433]
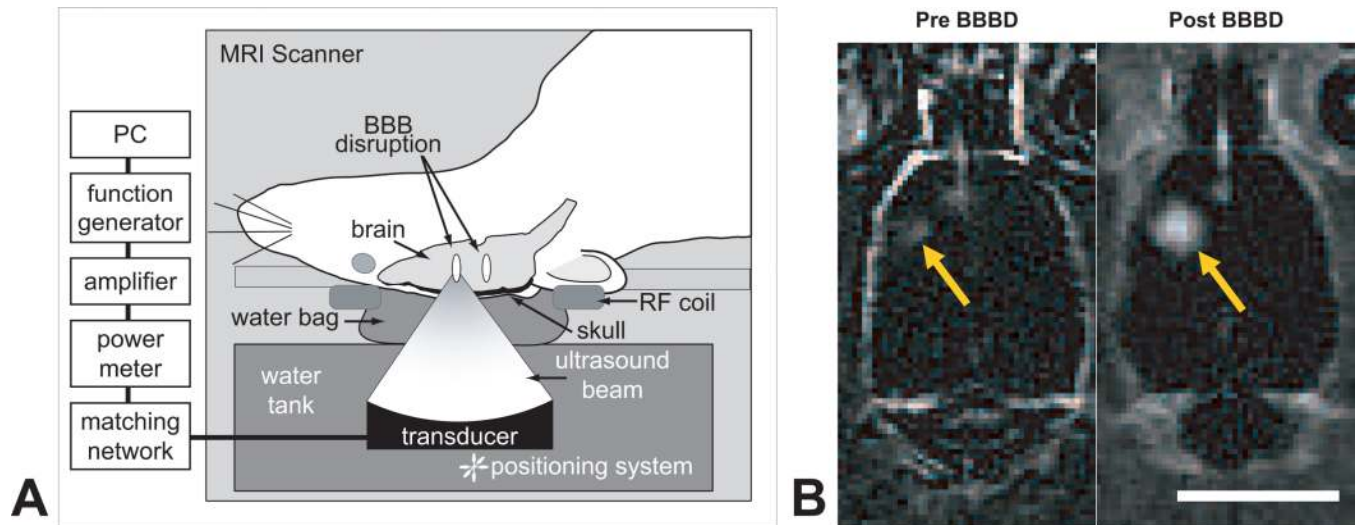
Fig. 1.
A, Experimental set-up for MRI-guided focused ultrasound-induced BBB disruption in rats with implanted 9L gliosarcoma. Pulsed ultrasound was focused in and around the tumor (Frequency: 1.7 MHz, Pressure: 1.2 MPa, Burst length: 10 ms, Repetition frequency: 1 Hz, Duration: 60–120 s; see ref (Treat et al. 2007) for further detail) with simultaneous i.v. administration of Definity microbubble ultrasonic contrast agent. *B,* Contrast-enhanced T1-weighted magnetic resonance images of the rat brain before (left) and after (right) ultrasound-induced BBB disruption around the tumor showed increased penetration of MR contrast agent through the BBB in the targeted area after sonication.
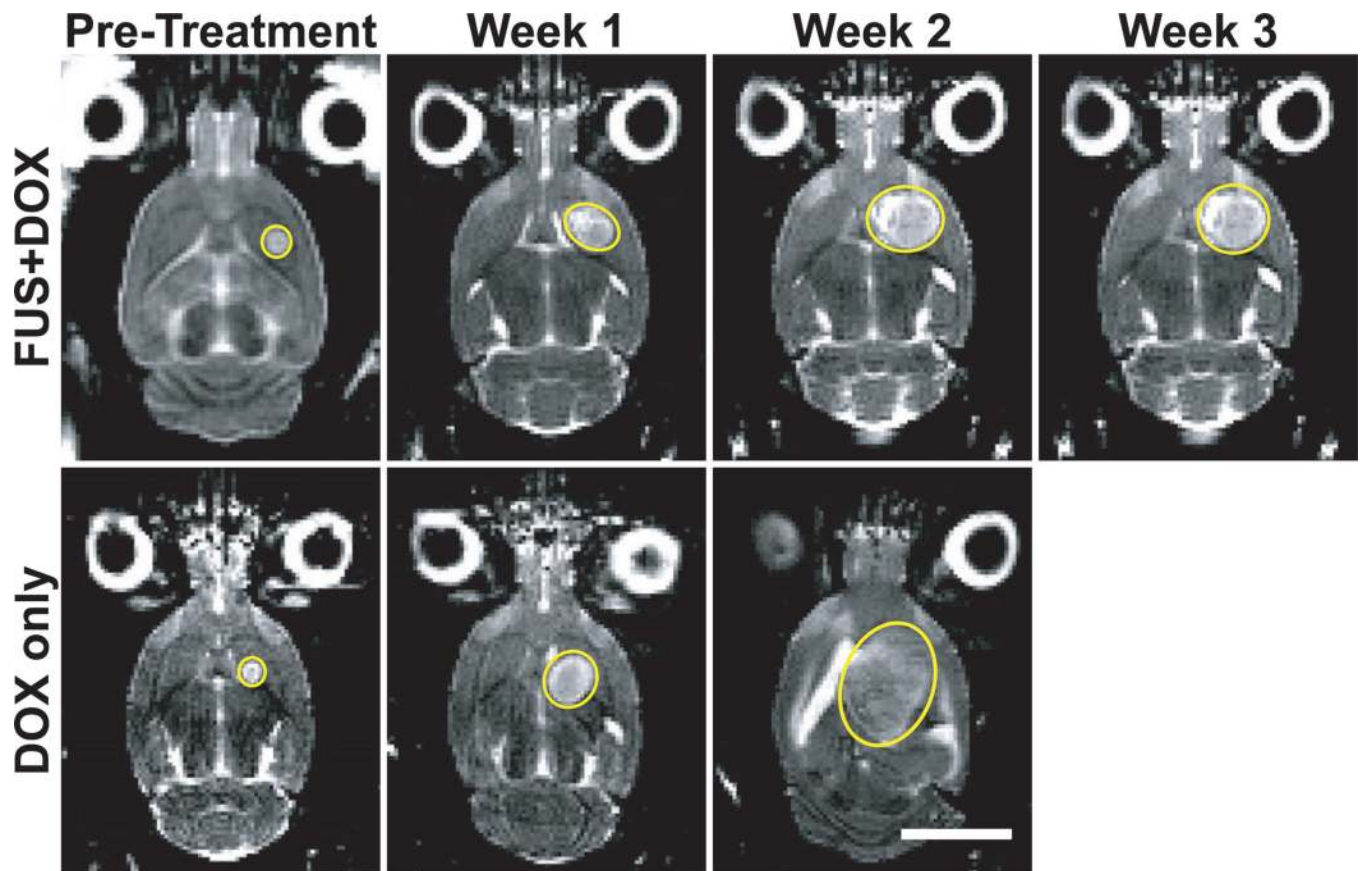
Fig. 2.
T2-weighted magnetic resonance images of a rat brain with implanted 9L gliosarcoma (outlined) before and 1, 2, and 3 weeks after treatment with focused ultrasound and i.v. liposomal doxorubicin (FUS+DOX; top row) or treatment with i.v. liposomal doxorubicin (DOX only; bottom row). While the tumor in the rat treated with DOX only continued to grow exponentially ($R^2 = 0.999$) even after treatment, tumor growth in the rat treated with FUS+DOX was visibly slowed in comparison.
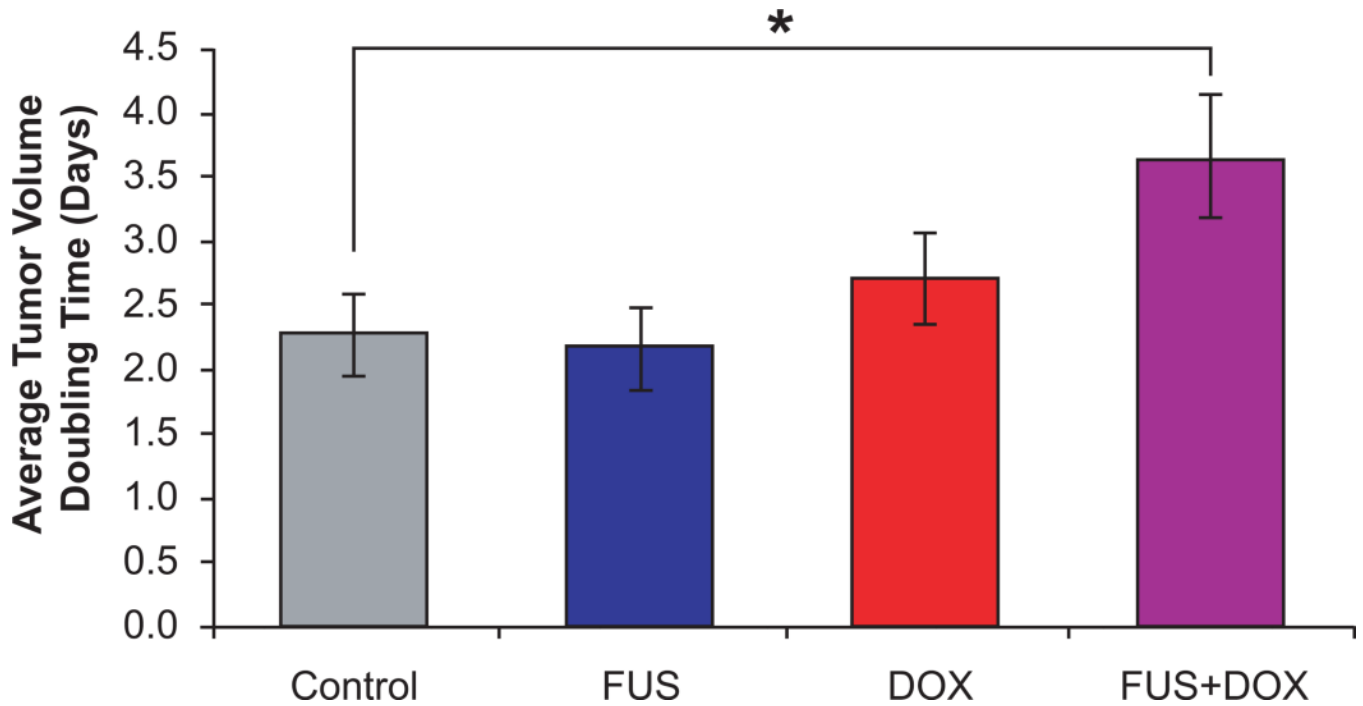
Fig. 3.
Average tumor volume doubling time in rats with intracranially implanted 9L gliosarcoma after treatment with one of the following: microbubble-enhanced focused ultrasound (FUS only), i.v. administration of 5.67 mg/kg liposomal doxorubicin (DOX only), or microbubble-enhanced focused ultrasound and i.v. administration of 5.67 mg/kg liposomal doxorubicin (FUS+DOX). Doubling time was calculated from exponential growth time constants determined from least-squares regression analyses. Rats treated with FUS+DOX had longer average tumor volume doubling times (3.7 ± 0.5 days) than any other group.
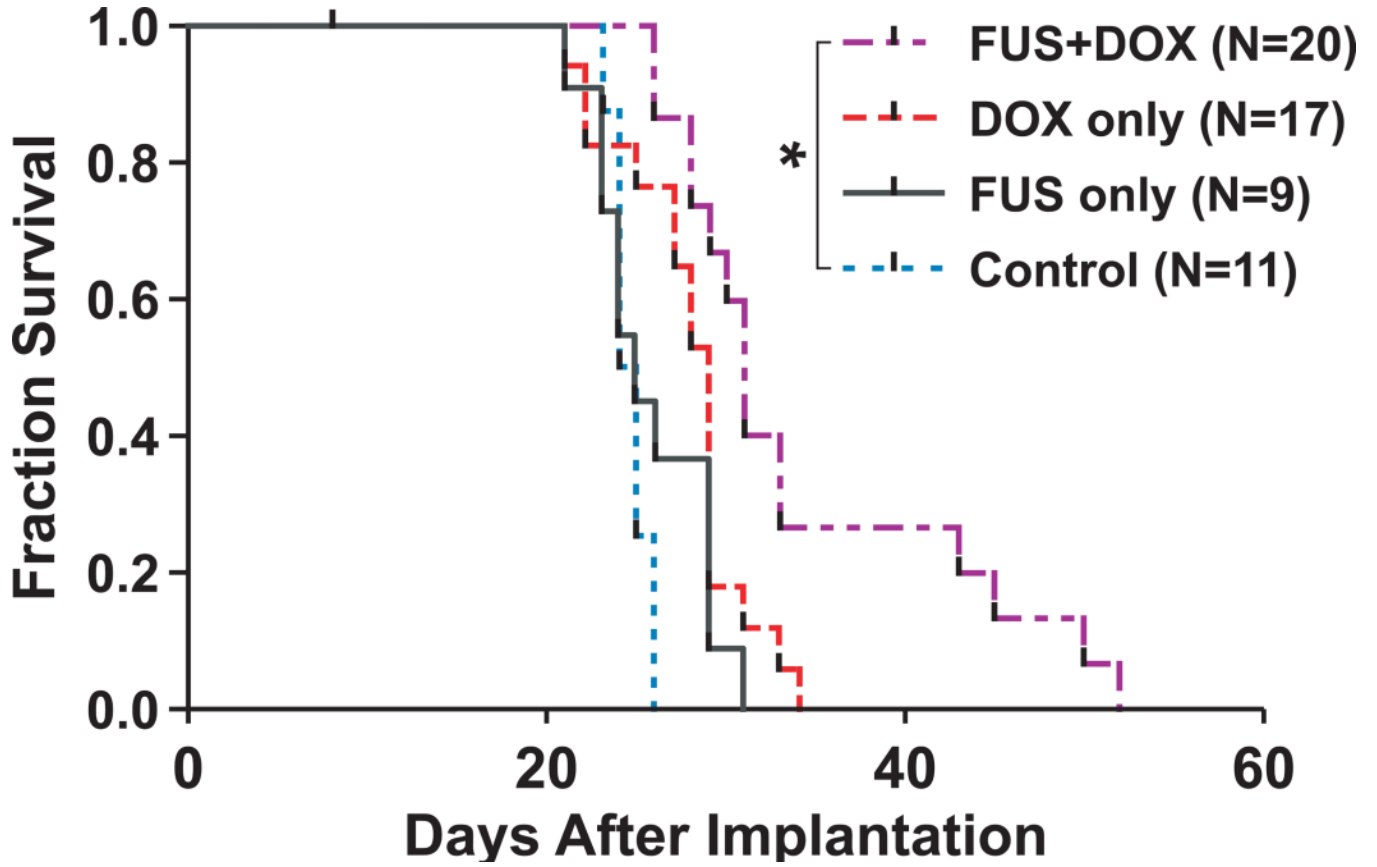
Fig. 4.
Fraction of survival (Kaplan-Meier plot) of rats with intracranially implanted 9L gliosarcoma after treatment on day 8 with one of preparations listed in Fig. 3. Rats which received a single treatment of FUS+DOX had a 24% greater median survival time than nontreated rats (Log-Rank $X^2 = 11.61$; $p = 0.0007$) and a greater proportion in long-term survivors; the other treatment groups were not significantly different from the control group.
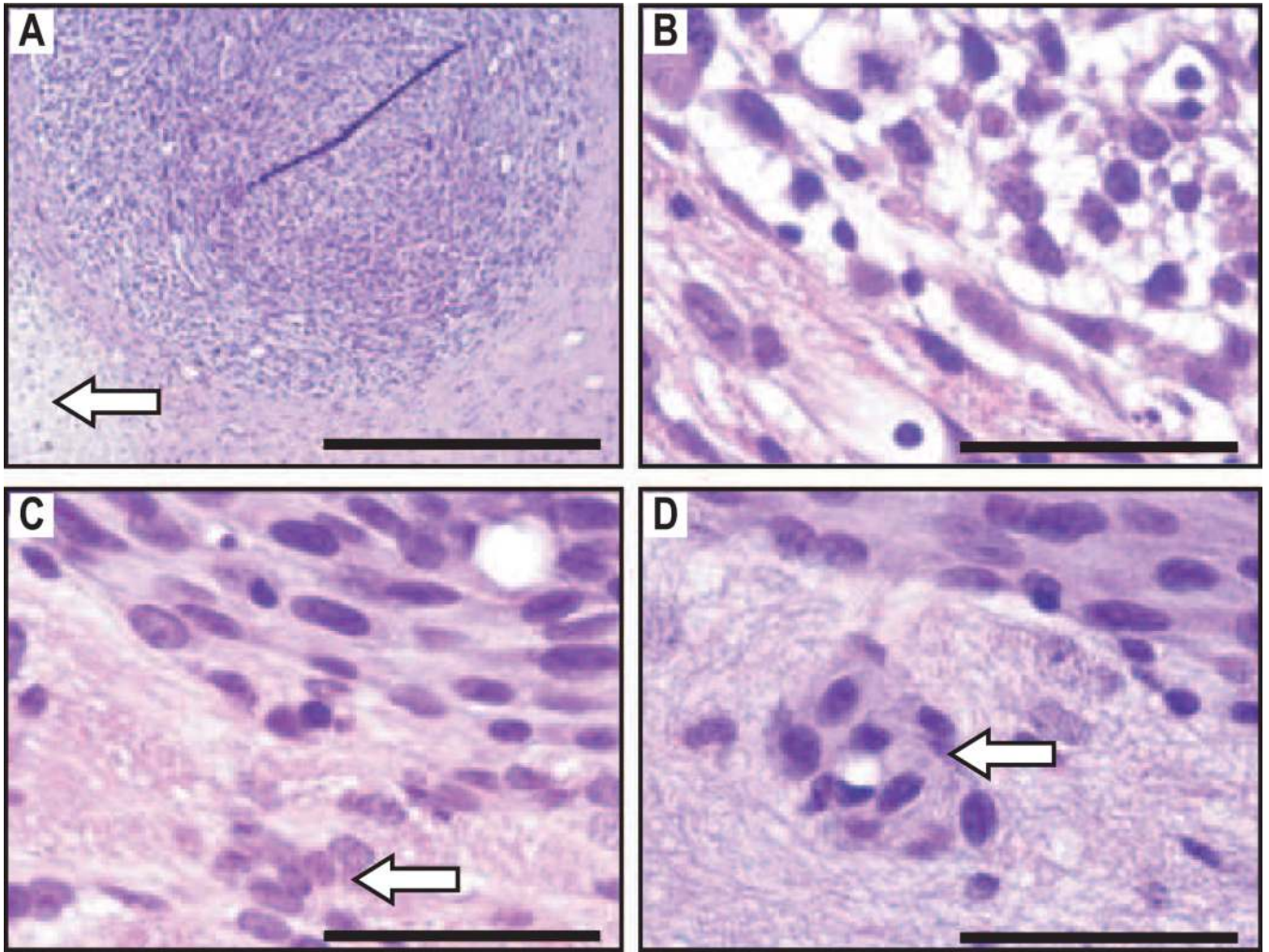
Fig. 5.
H&E-stained sections of rat brains with implanted 9L gliosarcoma 48 h after FUS+DOX treatment: *A*, Damage to gliosarcoma is noted in the peripheral region of the tumor and in the tissue beyond the tumor boundary (arrow); *B*, Detail of peripheral region of (*A*) showing parenchymal vacuolation and damaged tumor cells; *C* – *D*, Detail of a similar tumor in a rat treated with DOX only, showing intact tissue at the tumor edge and undamaged infiltrating tumor cells in the tissue beyond the solid tumor (*C*) and surrounding an intact blood vessel (*D*) (arrows). Scale bars: (*A*) 500 μm; (*B* – *D*) 50 μm.

Table 1

Results from survival analysis.

Treatment Group	Median Survival (d)	IST_{median} (%)[§]	P-value[§]	X^{2}[§]
No Treatment (N=11)	25	---	---	---
FUS-only (N=9)	25	0%	0.26	1.25
DOX-only (N=17)	29	16%	0.17	1.86
FUS+DOX (N=20)	31	24%	0.0007	11.61

IST_{median} Improvement in survival compared to the "No Treatment" group.

[§]Compared to the "No Treatment" group.